

Resorcinol Based Acyclic Dimeric and Cyclic Di- and Tetrameric Cyclodiphosphazanes: Synthesis, Structural Studies, and Transition Metal Complexes

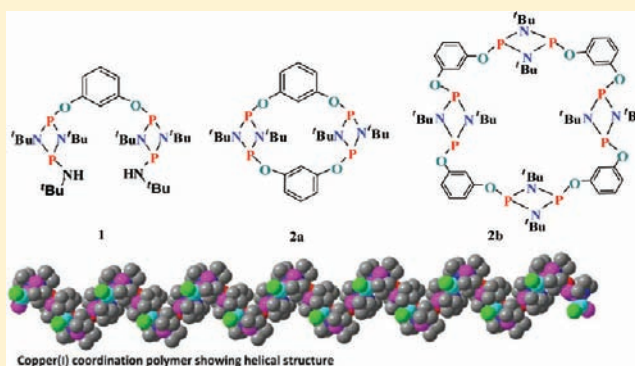
Guddekoppa S. Ananthnag,[†] Seema Kuntavalli,[†] Joel T. Mague,[‡] and Maravanji S. Balakrishna^{*†}

[†]Phosphorus Laboratory, Department of Chemistry, Indian Institute of Technology Bombay, Powai, Mumbai 400 076, India

[‡]Department of Chemistry, Tulane University, New Orleans, Louisiana 70118, United States

Supporting Information

ABSTRACT: The condensation reaction of resorcinol with *cis*-[ClP(μ -N^tBu)₂PN(H)^tBu] produced a difunctional derivative 1,3-C₆H₄[OP(μ -N^tBu)₂PN(H)^tBu]₂ (**1**), whereas the similar reaction with [ClP(μ -N^tBu)]₂ resulted in the formation of a 1:1 mixture of dimeric and tetrameric species, [P(μ -N^tBu)]₂{1,3-(O)₂-C₆H₄]₂ (**2a**) and [P(μ -N^tBu)]₄{1,3-(O)₂-C₆H₄]₄ (**2b**), which were separated by repeated fractional crystallization and column chromatography. The reaction of dimer **2a** with H₂O₂ and selenium produces tetrachalcogenides [P(μ -N^tBu)]₂{1,3-(O)₂-C₆H₄]₂ (**3**) and [SeP(μ -N^tBu)]₂{1,3-(O)₂-C₆H₄]₂ (**4**), respectively. The reaction between the dimer (**2a**) and [Pd(μ -Cl)(η ³-C₃H₅)]₂ or AuCl(SMe₂) yielded the corresponding tetranuclear complexes, [Cl(η ³-C₃H₅)PdP(μ -N^tBu)]₂{1,3-(O)₂-C₆H₄]₂ (**5**) and [ClAuP(μ -N^tBu)]₂{1,3-(O)₂-C₆H₄]₂ (**6**) in good yield. The complexes **5** and **6** are the rare examples of phosphorus macrocycles containing two or more exocyclic transition metal fragments. Treatment of **1** with copper halides in 1:1 molar ratio resulted in the formation of one-dimensional (1D) coordination polymers, [(CuX){1,3-C₆H₄{OP(μ -N^tBu)₂PN(H)^tBu}}]_n (**7**, X = Cl; **8**, X = Br; **9**, X = I), which showed the helical structure in solid state because of intramolecular hydrogen bonding, whereas similar reactions of **1** with 4 equiv of copper halides also produced 1D-coordination polymers, [(Cu₂X₂)₂{1,3-C₆H₄{OP(μ -N^tBu)₂PN(H)^tBu}}]_n (**10**, X = Cl; **11**, X = Br; **12**, X = I), but containing Cu₂X₂ rhomboids instead of CuX linkers. The crystal structures of **1**, **2a**, **2b**, **4**, **7–9**, and **12** were established by X-ray diffraction studies.



INTRODUCTION

The cyclodiphosphazanes or diazadiphosphetidines of the type [XP(μ -NR)]₂ have proved as both neutral and anionic ligands toward both main group and transition elements.¹ In addition, these four membered rings have been employed as building blocks in the formation of a range of inorganic macrocycles,² as mechanistic probes for organic reactions,³ and, in catalytic⁴ and biological applications.⁵ Planar geometry, preference for *cis*-conformation of phosphorus substituents, choice of metals, and selectivity in coordination modes make them versatile bridging ligands for the construction of polynuclear metalomacrocycles,⁶ chains, or one- (1D), two- (2D), and three-dimensional (3D) coordination polymers.⁷

Copper(I) halides, in particular cuprous iodide (CuI), display a wide range of structures (Chart 1) when coordinated to phosphorus based ligands. The coordination number of copper(I) is generally three or four and often the donor solvents occupy one of the coordination sites when copper(I) assumes open structure. Tertiary phosphines with moderate steric bulk when reacted with CuX, depending on the reaction conditions and the solvent employed, form either simple mono-

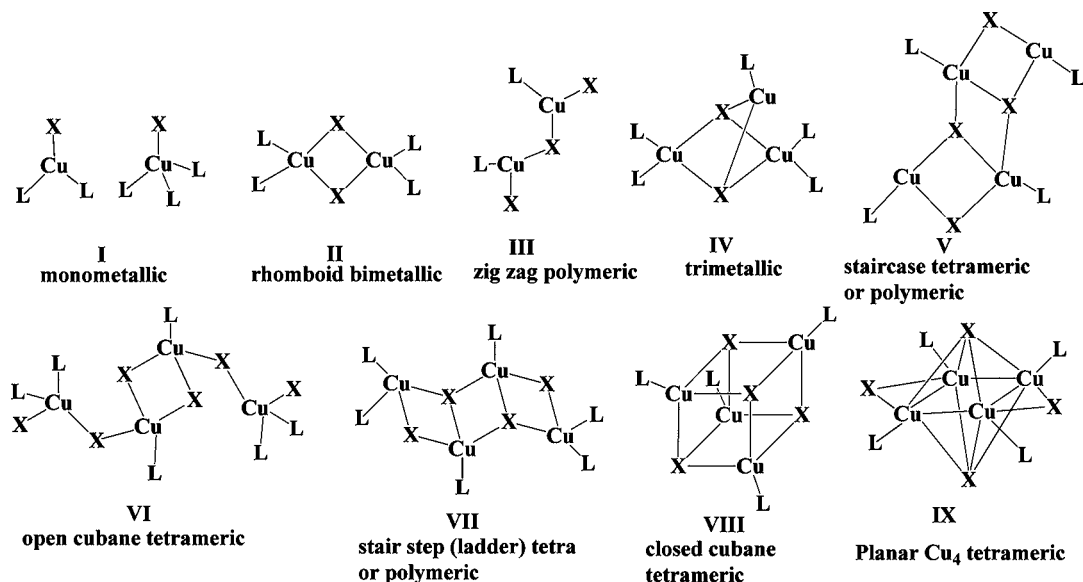
to trimetallic (I to IV)⁸ or tetrametallic cuboid complexes of the type VIII,⁹ whereas the short-bite bis(phosphine)s prefer ladder (V), stair step tetrameric (VII), or 1D-coordination polymeric (VII) structures.¹⁰ Some bidentate ligands have also shown an unusual tetrameric structure of the type IX with all the four copper atoms in one plane.¹¹

Recently we have investigated the Group 11 metal chemistry of a few derivatives of cyclodiphosphazanes. The interaction of cyclodiphosphazanes with copper halides in η^1 fashion led to the formation of mononuclear copper complexes (X), whereas the bridged bidentate mode afforded oligomeric (XI) or polymeric structures (XII), with P₂N₂ rings and rhomboid Cu₂X₂ units linked alternatively.¹² So far, the stoichiometry controlled reactions have yielded products of the type X–XII, and to get some insight into the various building blocks that can be generated during molecular assembly, attempts are being made to synthesize the products of the type XII and XIV. Herein, we report the synthesis, structural characterization,

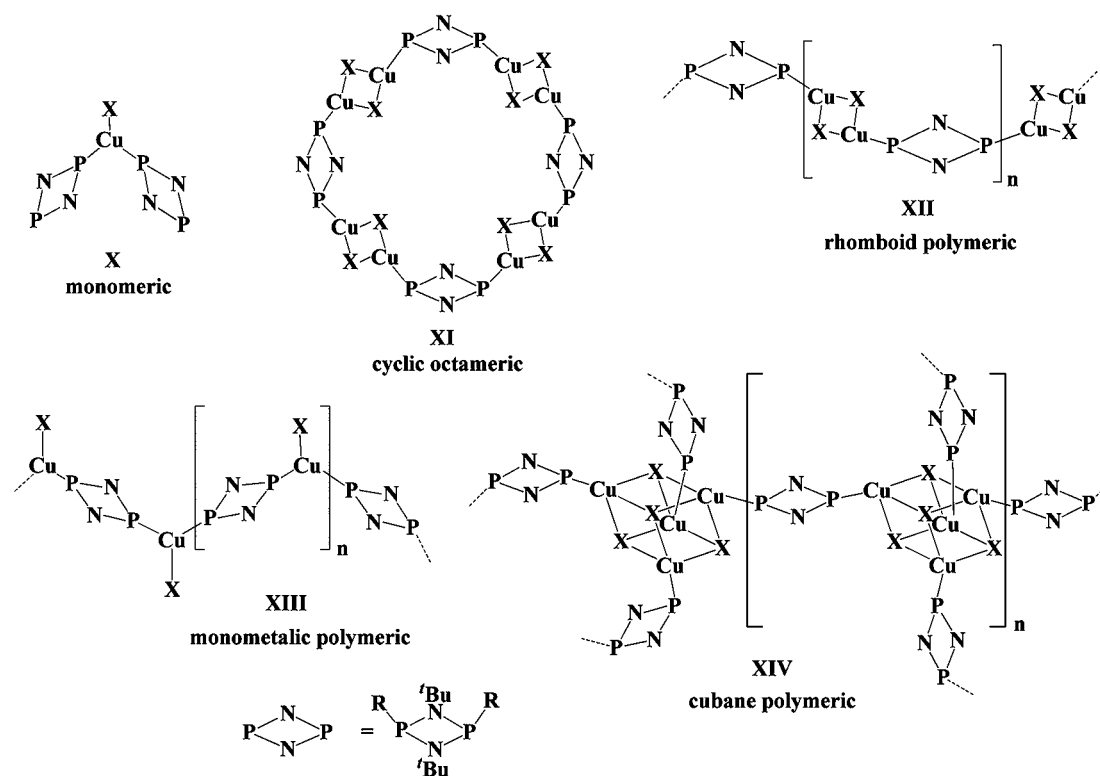
Received: March 13, 2012

Published: May 7, 2012

Chart 1. Possible Structural Motifs for Copper(I) Halide-Soft Ligand Complexes



structural motifs for copper(I) halide-phosphine complexes



structural motifs for copper(I) halide-cyclodiphosphazane complexes

(L = monodentate ligand; LL = bidentate ligand (with both μ - and η^1 - possibilities); X = halides)

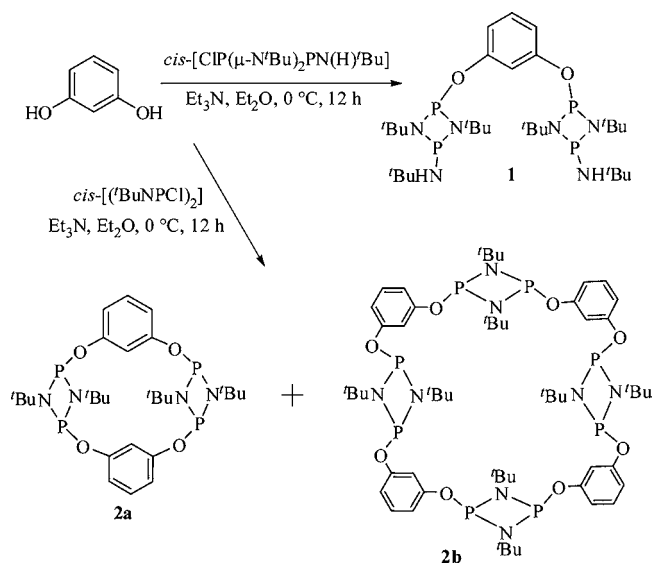
oxidation reactions, and coordination behavior of a dimeric acyclic cyclodiphosphazane as well as dimeric and tetrameric macrocycles of cyclodiphosphazanes derived from resorcinol.

RESULTS AND DISCUSSION

Synthesis of $1,3\text{-C}_6\text{H}_4[\text{OP}(\mu\text{-N}^t\text{Bu})_2\text{PN}(\text{H})^t\text{Bu}]_2$ (1). Recently, we reported the synthesis of an acyclic dimer of cyclodiphosphazane $[\text{CH}_2\text{OP}(\mu\text{-N}^t\text{Bu})_2\text{PN}(\text{H})^t\text{Bu}]_2$ by the reaction of $\text{cis-}[\text{ClP}(\mu\text{-N}^t\text{Bu})_2\text{PN}(\text{H})^t\text{Bu}]$ with ethylene gly-

col.¹³ A similar derivative of cyclodiphosphazane, $1,3\text{-C}_6\text{H}_4[\text{OP}(\mu\text{-N}^t\text{Bu})_2\text{PN}(\text{H})^t\text{Bu}]_2$ (**1**) (Scheme 1), having rigid aromatic backbone was obtained by the reaction of $\text{cis-}[\text{ClP}(\mu\text{-N}^t\text{Bu})_2\text{PN}(\text{H})^t\text{Bu}]$ with resorcinol in diethyl ether in the presence of triethyl amine at 0°C as a white crystalline solid in good yield. The ligand **1** is moderately air stable and soluble in most of the organic solvents. The ^{31}P NMR spectrum of **1** exhibits two singlets at 100.1 and 129.7 ppm, for amino-P (hereafter “outer”) and aryloxo-P (hereafter “inner”) atoms,

Scheme 1



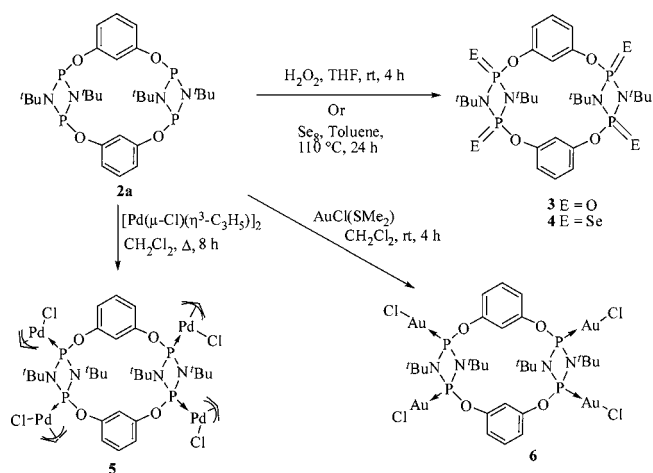
respectively. In the ^{13}C NMR spectrum two virtual triplets at 52.2 ($^2J_{\text{PC}} = 13.1$ Hz) and 31.5 ppm ($^3J_{\text{PC}} = 6.3$ Hz) were assigned to *tert*-butyl groups on endocyclic nitrogen atoms, whereas two doublets at 51.5 ($^2J_{\text{PC}} = 14.1$ Hz) and 32.9 ppm ($^3J_{\text{PC}} = 9.2$ Hz) were assigned to *tert*-butyl groups attached to exocyclic nitrogen atoms. The mass spectrum of **1** shows the molecular ion peak at m/z 661.1 ($M+1$). Further evidence for structure and molecular composition of **1** came from ^1H NMR spectrum, microanalysis, and single-crystal X-ray diffraction study.

Dimeric and Tetrameric Derivatives: $[\{\text{P}(\mu\text{-N}^t\text{Bu})\}_2\{1,3\text{-}(\text{O})_2\text{-C}_6\text{H}_4\}_2]$ (**2a**) and $[\{\text{P}(\mu\text{-N}^t\text{Bu})\}_2\{1,3\text{-}(\text{O})_2\text{-C}_6\text{H}_4\}_4]$ (**2b**). The condensation of $[\text{CIP}(\mu\text{-N}^t\text{Bu})_2]$ with bifunctional organic alcohols, amines, or amino-alcohols ($\text{LL}'\text{H}_2$), produce a broad range of macrocycles $[\{\text{P}(\mu\text{-N}^t\text{Bu})\}_2(\text{LL}')_n]$ ($n = 1\text{--}5$).¹⁴ The size of the macrocycle depends largely on the size, position of reaction site and orientation of the organic linker (see Supporting Information, Chart S1). Reaction conditions also play a significant role in producing selectivity. Monomers are generally formed with more flexible organic spacers, while rigid organic spacers favor higher oligomers. The reaction of $cis\text{-}[\text{CIP}(\mu\text{-N}^t\text{Bu})_2]$ with resorcinol in diethyl ether at $0\text{ }^\circ\text{C}$, in the presence of triethyl amine afforded a mixture of dimeric and tetrameric compounds, $[\{\text{P}(\mu\text{-N}^t\text{Bu})\}_2\{1,3\text{-}(\text{O})_2\text{-C}_6\text{H}_4\}_2]$ (**2a**) and $[\{\text{P}(\mu\text{-N}^t\text{Bu})\}_2\{1,3\text{-}(\text{O})_2\text{-C}_6\text{H}_4\}_4]$ (**2b**) (Scheme 1), along with a small quantity of hydrolyzed and oxidized products, substantiated by ^{31}P NMR spectroscopic data. Repeated fractional crystallization from toluene resulted in the isolation of dimer **2a** in low yield. The separation of tetramer by the same method was unsuccessful as it was always contaminated with small percentage of dimer cocrystallizing with the tetramer. The attempts to separate the crystals have also been unsuccessful because of the similar crystal morphology. However, the mixture containing **2a** and **2b** on passing through a silica gel column, using *n*-hexanes and dichloromethane as eluent, under nitrogen atmosphere followed by recrystallization from toluene gave both the compounds **2a** and **2b** in pure form, from the respective fractions. The ^{31}P NMR spectrum of **2a** shows a single resonance at 131.5 ppm. In the ^1H NMR spectrum of **2a**, a singlet was observed at 1.27 ppm for *tert*-butyl groups. The ^{31}P NMR spectrum of **2b** shows a single

resonance at 146.0 ppm. In the ^1H NMR spectrum, a singlet was observed at 1.35 ppm for *tert*-butyl groups of **2b**. The elemental analysis data of **2a** and **2b** were in accordance with the proposed structures. The structures of **2a** and **2b** were further confirmed by single-crystal X-ray diffraction studies.

Oxidation Reactions of $[\{\text{P}(\mu\text{-N}^t\text{Bu})\}_2\{1,3\text{-}(\text{O})_2\text{-C}_6\text{H}_4\}_2]$ (2a**).** The reaction of $[\{\text{P}(\mu\text{-N}^t\text{Bu})\}_2\{1,3\text{-}(\text{O})_2\text{-C}_6\text{H}_4\}_2]$ (**2a**) with H_2O_2 in tetrahydrofuran (THF) at room temperature leads to the oxidation of all the four phosphorus atoms to give $[\{(\text{O})\text{P}(\mu\text{-N}^t\text{Bu})\}_2\{1,3\text{-}(\text{O})_2\text{-C}_6\text{H}_4\}_2]$ (**3**) in quantitative yield. The ^{31}P NMR spectrum of **3** shows a singlet at -11.9 ppm. The reaction of **2a** with 4 equiv of selenium in toluene under refluxing condition furnished the tetrakis(selenide), $[\{(\text{Se})\text{P}(\mu\text{-N}^t\text{Bu})\}_2\{1,3\text{-}(\text{O})_2\text{-C}_6\text{H}_4\}_2]$ (**4**), in good yield (Scheme 2). The ^{31}P NMR spectrum of **4** exhibits a singlet at 32.7 ppm with ^{77}Se satellites attributed to the AA'X spin system typical for selenide derivatives of *cis*-cyclodiphosphazanes. The $^1J_{\text{PSe}}$ is 996 Hz, whereas the $^2J_{\text{PP}}$ is 7.3 Hz. The coupling constants were comparable to that found in *cis*- $[\text{tBuNP}(\text{Se})(\text{OCH}_2\text{CH}_2\text{OMe})_2]$ ($^1J_{\text{PSe}} = 953$ Hz, $^2J_{\text{PP}} = 6.7$ Hz), *cis*- $[\text{tBuNP}(\text{Se})(\text{OCH}_2\text{CH}_2\text{SMe})_2]$ ($^1J_{\text{PSe}} = 954$ Hz, $^2J_{\text{PP}} = 6.8$ Hz)¹⁵ and *cis*- $[\text{tBuNP}(\text{Se})(\text{OMe})_2]$ ($^1J_{\text{PSe}} = 954.5$ Hz, $^2J_{\text{PP}} = 8.0$ Hz).¹⁶ The structure of **4** was confirmed by single-crystal X-ray structure determination.

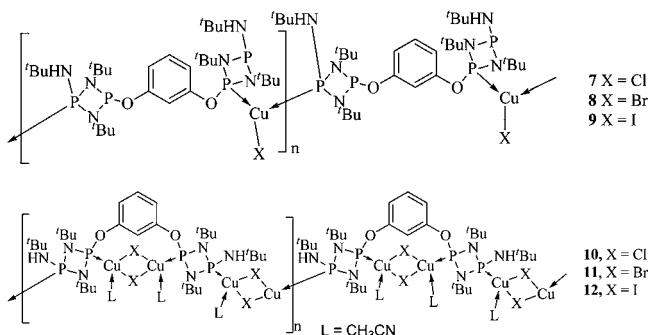
Scheme 2



$[\{\text{P}(\mu\text{-N}^t\text{Bu})\}_2\{1,3\text{-}(\text{O})_2\text{-C}_6\text{H}_4\}_2]$ (**4**), in good yield (Scheme 2). The ^{31}P NMR spectrum of **4** exhibits a singlet at 32.7 ppm with ^{77}Se satellites attributed to the AA'X spin system typical for selenide derivatives of *cis*-cyclodiphosphazanes. The $^1J_{\text{PSe}}$ is 996 Hz, whereas the $^2J_{\text{PP}}$ is 7.3 Hz. The coupling constants were comparable to that found in *cis*- $[\text{tBuNP}(\text{Se})(\text{OCH}_2\text{CH}_2\text{OMe})_2]$ ($^1J_{\text{PSe}} = 953$ Hz, $^2J_{\text{PP}} = 6.7$ Hz), *cis*- $[\text{tBuNP}(\text{Se})(\text{OCH}_2\text{CH}_2\text{SMe})_2]$ ($^1J_{\text{PSe}} = 954$ Hz, $^2J_{\text{PP}} = 6.8$ Hz)¹⁵ and *cis*- $[\text{tBuNP}(\text{Se})(\text{OMe})_2]$ ($^1J_{\text{PSe}} = 954.5$ Hz, $^2J_{\text{PP}} = 8.0$ Hz).¹⁶ The structure of **4** was confirmed by single-crystal X-ray structure determination.

Palladium and Gold Complexes. Treatment of $[\text{Pd}(\mu\text{-Cl})(\eta^3\text{-C}_3\text{H}_5)_2]$ with **2a** in 2:1 molar ratio in dichloromethane under reflux conditions gave a tetra-palladium complex $[\{(\text{Cl})(\eta^3\text{-C}_3\text{H}_5)\text{PdP}(\mu\text{-N}^t\text{Bu})\}_2\{1,3\text{-}(\text{O})_2\text{-C}_6\text{H}_4\}_2]$ (**5**) in good yield. The reaction between **2a** and 4 equiv of $[\text{AuCl}(\text{SMe}_2)]$ in dichloromethane resulted in the formation of tetragold complex $[\{(\text{ClAu})\text{P}(\mu\text{-N}^t\text{Bu})\}_2\{1,3\text{-}(\text{O})_2\text{-C}_6\text{H}_4\}_2]$ (**6**). The ^{31}P NMR spectrum of **5** shows two broad singlets at 122.7 and 115.0 ppm which may be due to the improper folding of dimeric macrocycle after complexation. Because of the poor solubility of complex **5**, low-temperature NMR studies could not be carried out. In contrast, the ^{31}P NMR spectrum of **6** shows a single resonance at 98.4 ppm indicating the symmetrical nature of all phosphorus atoms. In the ^1H NMR spectrum *tert*-butyl groups show a singlet at 1.57 ppm. The ^1H assignments and microanalysis data are found to be consistent with the proposed structures in all cases.

Synthesis of Copper(I) Complexes. The treatment of 1 equiv of copper halide (CuCl, CuBr, or CuI) with ligand **1** in a 1:1 mixture of dichloromethane and acetonitrile yielded coordination polymers $[\{1,3\text{-C}_6\text{H}_4(\text{OP}(\mu\text{-N}^t\text{Bu})_2\text{PN}(\text{H})^t\text{Bu})_2\}(\text{CuX})]_n$ (**7**, X = Cl; **8**, X = Br; **9**, X = I) in good yield. The complexes were precipitated from the reaction mixture as insoluble white solids. In these polymers, copper centers are found to be coordinated by one inner and one outer phosphorus atom from two cyclodiphosphazanes in a zigzag fashion. The ^{31}P NMR spectra of **7–9** are identical and show four broad signals in the range of 139.4–67.2 ppm, indicating the presence of four different types of phosphorus centers in each complex. For example, in case of **7**, single resonances at 135.6 ppm and 98.7 ppm are assigned respectively to uncoordinated inner-phosphorus and coordinated inner-phosphorus, while high field signals at 73.8 and 67.2 ppm are assigned, to uncoordinated and coordinated outer-phosphorus centers, respectively. The product formation was found to be independent of stoichiometry of the reactants as both 1:1 and 1:2 reactions led to the formation of the same product. Because of the poor solubility of all the polymeric compounds and the presence of quadrupolar nuclei, all the peaks in ^{31}P NMR spectra appeared broad, and low temperature NMR studies could not be carried out.



The treatment of ligand **1** with 4 equiv of copper halide (CuCl, CuBr or CuI) produced copper(I) coordination polymers $[\{1,3\text{-C}_6\text{H}_4(\text{OP}(\mu\text{-N}^t\text{Bu})_2\text{PN}(\text{H})^t\text{Bu})_2\}(\text{Cu}_2(\mu\text{-X})_2)]_n$ (**10**, X = Cl; **11**, X = Br; **12**, X = I). The compounds **10–12** are poorly soluble in most of the organic solvents, but partially soluble in hot dimethylsulfoxide (DMSO). In the coordination polymers **10–12**, one $[\text{Cu}_2(\mu\text{-X})_2]$ rhombic unit is coordinated by two inner phosphorus atoms, whereas the two outer phosphorus atoms from two cyclodiphosphazane ligands are held together by $[\text{Cu}_2(\mu\text{-X})_2]$ units resulting in the formation of 1D-coordination polymers. The ^{31}P NMR spectra of **10–12** show three broad resonances in the range of 66.2–107.9 ppm. For example, in case of **10**, a signal at 107.9 ppm is assigned to coordinated inner-phosphorus atoms and broad resonances at 80.0 and 66.5 ppm are assigned to coordinated outer-phosphorus atoms. The polymeric structures of complexes **7–9** and **12** in the solid state have been revealed by the X-ray diffraction studies.

Molecular Structures of Compounds 1, 2a, 2b, 4, 7–9, and 12. Perspective views of the molecular structures of all compounds with the atom numbering schemes are shown in Figures 1–9. Crystal data and the details of the structure determinations are given in Table 1 while the selected bond lengths and the interbond angles appear in Tables 2 and 3.

The crystals suitable for X-ray diffraction study were obtained from toluene solution of **1** at -20°C . Normally the longer P–

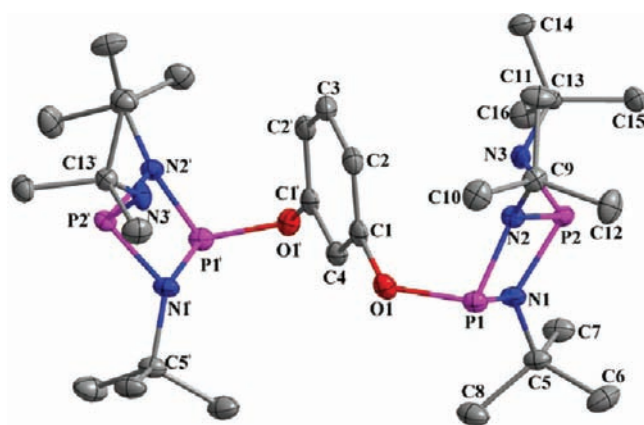


Figure 1. Molecular structure of $[\{1,3\text{-C}_6\text{H}_4\text{OP}(\mu\text{-N}^t\text{Bu})_2\text{PN}(\text{H})^t\text{Bu})_2\}(\text{CuX})]_n$ (**1**). Thermal ellipsoids are drawn at the 50% probability level. Hydrogen atoms have been omitted for clarity. Symmetry operations (i) $-x, -y, -z$ (ii) $1/2-x, 1/2-y, -z$.

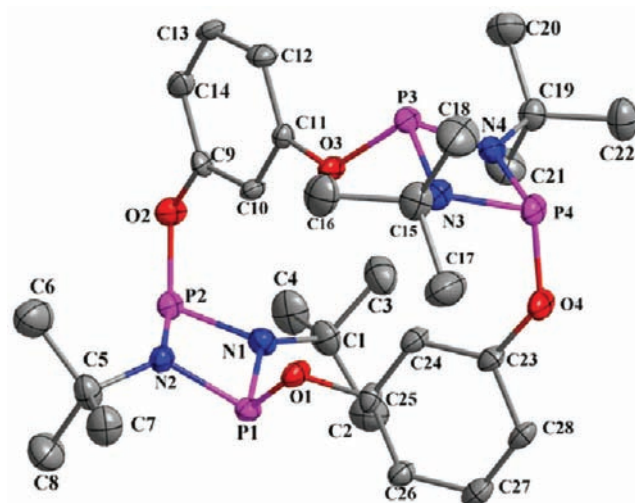


Figure 2. Molecular structure of $[\{P(\mu\text{-N}^t\text{Bu})\}_2\{1,3\text{-(O)}_2\text{-C}_6\text{H}_4\}]_2$ (**2a**). Thermal ellipsoids are drawn at the 50% probability level. All hydrogen atoms have been omitted. Symmetry operation (i) $-x, -y, -z$.

N bonds are associated with phosphorus atom having an exocyclic nitrogen substituent, whereas phosphorus bearing oxo-, alkoxy-, aryloxy-, or halo- substituents show shorter P–N bond distances.¹⁷ The average endocyclic P–N bond distance of phosphorus bearing an aryloxy- substituent is 1.697 Å, whereas the average P–N bond distance, where phosphorus is bound to exocyclic nitrogen is 1.738 Å. The exocyclic P2–N3 bond distance [1.6480(15) Å] is shorter than endocyclic P–N bond distances. The exocyclic P–N distances are always shorter and comparable with typical P–N distances observed in both cyclic and acyclic diphosphazanes.^{1d} The P1–O1 bond distance in **1** [1.6705(13) Å] is slightly longer than that found in $[\text{CH}_2\text{OP}(\mu\text{-N}^t\text{Bu})_2\text{PN}(\text{H})^t\text{Bu})_2]$ ¹³ [1.6383(14) Å], $\text{Et}_2\text{C}[\text{CH}_2\text{OP}(\mu\text{-N}^t\text{Bu})_2\text{PN}(\text{H})^t\text{Bu})_2]$ [1.629(2) Å], and $\text{C}[\text{CH}_2\text{OP}(\mu\text{-N}^t\text{Bu})_2\text{PN}(\text{H})^t\text{Bu})_4]$ ^{2e} [1.630(4) Å], but comparable with the same in $[\text{Bu}(\text{H})\text{NP}(\mu\text{-N}^t\text{Bu})_2\text{POC}_6\text{H}_4\text{PPh}_2\text{-}o]$ [1.6881(11) Å].¹⁸ The P₂N₂ rings in **1** are puckered with a folding along N···N axis, as indicated by the dihedral angle between the corresponding N–P–N planes [$\sim 8.1^\circ$].

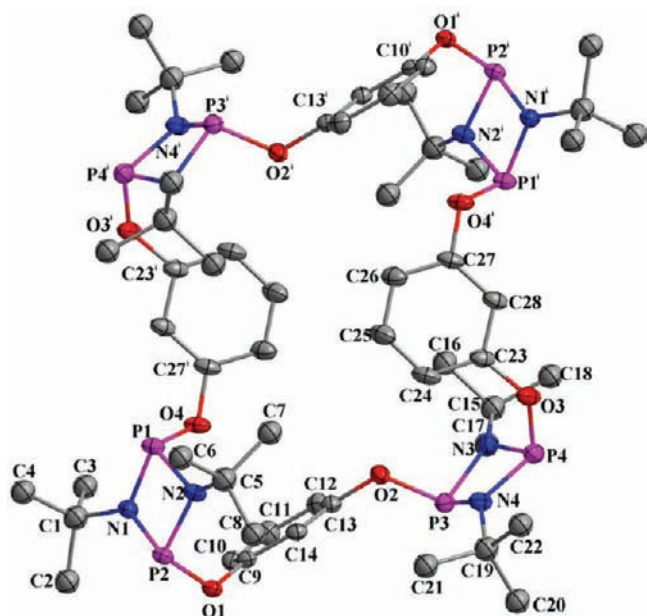


Figure 3. Molecular structure of $[\{P(\mu\text{-N}^t\text{Bu})\}_2\{1,3\text{-(O)}_2\text{-C}_6\text{H}_4\}]_4$ (**2b**). Thermal ellipsoids are drawn at the 50% probability level. Hydrogen atoms have been omitted for clarity. Symmetry operation (i) $-x, -y, -z$.

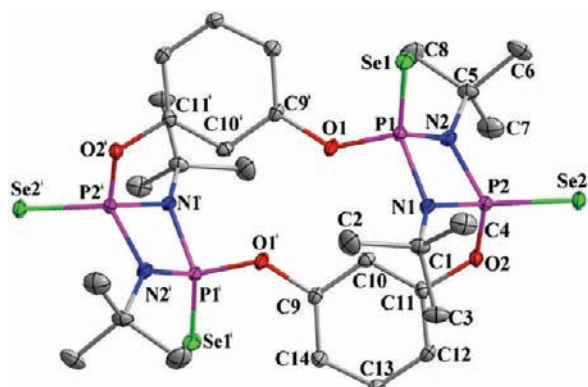


Figure 4. Molecular structure of $[\{(\text{Se})P(\mu\text{-N}^t\text{Bu})\}_2\{1,3\text{-(O)}_2\text{-C}_6\text{H}_4\}]_2$ (**4**). Thermal ellipsoids are drawn at the 50% probability level. All hydrogen atoms have been omitted. Symmetry operation (i) $-x, -y, -z$.

The low temperature X-ray diffraction studies unambiguously established the structures of **2a** and **2b**. The compounds **2a** and **2b** crystallize in the monoclinic crystal system. The structure of **2a** is similar to that previously reported $[\{P(\mu\text{-N}^t\text{Bu})\}_2\{2,6\text{-(NH)}_2\text{C}_5\text{H}_3\text{N}\}]_2$ by Wright and co-workers.⁵ The two P_2N_2 rings in **2a** are nearly parallel to each other as indicated by the angle between the mean planes of two rings $[3.375^\circ]$. The mean planes of alternative P_2N_2 rings are also parallel to each other in **2b**. The cavity of **2b** measures 11.22 \AA (mean) between the centroids of the alternative P_2N_2 ring units. The P_2N_2 rings are slightly puckered as indicated by their dihedral angles between the corresponding N-P-N planes in **2a** $[11.4^\circ]$ and **2b** $[6.9^\circ$ and $13.5^\circ]$. The average P-O bond distances in **2a** $[1.658 \text{ \AA}]$ and **2b** $[1.661 \text{ \AA}]$ are similar and comparable with those in $\{2,2'\text{-C}_{10}\text{H}_6\text{O}\}_2\{P(\mu\text{-N}^t\text{Bu})\}_2$ $[1.664 \text{ \AA}]$ ^{2b} and $[\{P(\mu\text{-N}^t\text{Bu})\}_2(\mu\text{-O})]_4$ $[1.654(2)\text{--}1.665(2) \text{ \AA}]$.¹⁹ The P-N bond lengths in **2a** $[1.697(4)\text{--}1.724(4) \text{ \AA}]$ and **2b** $[1.7001(14)\text{--}1.7204(5) \text{ \AA}]$ and P-N-P bond angles in **2a**

$[97.64(19)\text{--}97.9(2)^\circ]$ and **2b** $[97.33(7)\text{--}98.27(7)^\circ]$ are almost identical and similar to those of $[\{P(\mu\text{-N}^t\text{Bu})\}_2(\mu\text{-O})]_4$ $[\text{P-N}, 1.700(2)\text{--}1.732(2) \text{ \AA}$ and $\text{P-N-P}, 96.73(9)\text{--}99.2(1)^\circ]$.

The X-ray quality crystals of **4** were obtained from dichloromethane/pet-ether solution of **4** at room temperature. The structural features of **4** are similar to its starting compound **2a**. The mean planes of two aromatic rings and P_2N_2 rings are parallel to each other. The average P-O and P-N bond distances in **4** are 1.601 \AA and 1.685 \AA , are shorter than those of P(III) derivative, **2a**. Similar trends, that is, shrinking of P-O and P-N distances from P^{III} derivative to P^{V} derivative were observed in the analogues $[(2,2'\text{-C}_{10}\text{H}_6\text{O})\{(\text{O})P(\mu\text{-N}^t\text{Bu})\}_2]^{2b}$ and $[\text{tBuHN}(\text{tBuNP}(\text{Se}))_2\text{OCH}_2]_2$.¹³

Crystals of **7-9** and **12** suitable for X-ray diffraction were obtained by slow diffusion of copper halide solution in acetonitrile into a dichloromethane solution of **1** at room temperature. The compounds **7** and **9** crystallize in the orthorhombic crystal system, whereas **8** crystallizes in the monoclinic crystal system. The unit cell of the complex **7** contains two independent half molecules, with similar bonding properties. All copper atoms in **7-9** are tricoordinated and adopt a distorted trigonal planar geometry. The copper centers are coordinated by the inner phosphorus of one molecule and the outer phosphorus of other molecule of ligand, forming 1D coordination polymers. The tricoordinated copper centers in **7-9** are planar as suggested by the sum of the bond angles around copper centers (359.9°) in all the three cases. The Cu-P and Cu-X bond lengths are in good agreement with the literature values for tricoordinated copper(I)-phosphine complexes.²⁰ The P1-Cu-P3 bond angles in **7** $[119.30(5)^\circ]$, **8** $[118.24(3)^\circ]$, and **9** $[120.13(6)^\circ]$ are similar, and they indicate little or no influence of halogen atoms on the geometry around copper. The P1-Cu-P3 bond angles in **7-9** are less than the P-Cu-P bond angles reported in literature for tricoordinated copper complexes of both less bulkier phosphine ligands such as PPh_3 $[125.48(7)^\circ]$ ²¹ and bulkier ligands such as *cis*- $[\text{tBuNP}(\text{OC}_6\text{H}_4\text{OMe-o})]_2$ $[130.11(2)^\circ]$, PCy_3 $[134.44(8)^\circ]$,²⁰ and PBN_3 $[136.53(2)^\circ]$.²² This is due to the intramolecular hydrogen bonding between N-H and oxygen atom (see Supporting Information, Figure S1). The hydrogen bond distance in **8** is $2.0834(19) \text{ \AA}$ and the $\text{N-H}\cdots\text{O}$ bond angle is 163.53° ; similarly, in case of **7** and **9**, the hydrogen bond distances are $2.2697(27) \text{ \AA}$ and $2.1752(36) \text{ \AA}$, and the $\text{N-H}\cdots\text{O}$ bond angles are 169.40° and 164.34° , respectively. The intramolecular hydrogen bonding not only reduces the P1-Cu-P3 bond angle but it has greater effect on the solid state structure of these complexes as it guides the polymers to form a helical structure as shown in Figure 9.

The structure of polymer **12** consists of two different rhombic $[\text{Cu}_2(\mu\text{-I})_2]$ cores in it. In the $[\text{Cu1}(\mu\text{-I1,I2})\text{Cu2}]$ dimeric unit, one of the copper centers is tricoordinated with the coordination sites occupied by outer phosphorus atom of the cyclodiphosphazane and two bridging iodide atoms whereas the other copper center in the same unit is tetracoordinated, as acetonitrile occupies the fourth coordination site. The tricoordinated copper center, Cu2 adopts trigonal planar geometry, whereas the tetracoordinated copper center, Cu1 , adopts a distorted tetrahedral geometry. Since there are unsymmetrical interactions between the N-H hydrogen and iodide atoms, all the four Cu-I bond lengths differ significantly and can be roughly grouped into two sets with the longer distances $[2.6910(8)$ and $2.8168(6) \text{ \AA}]$ being associated with

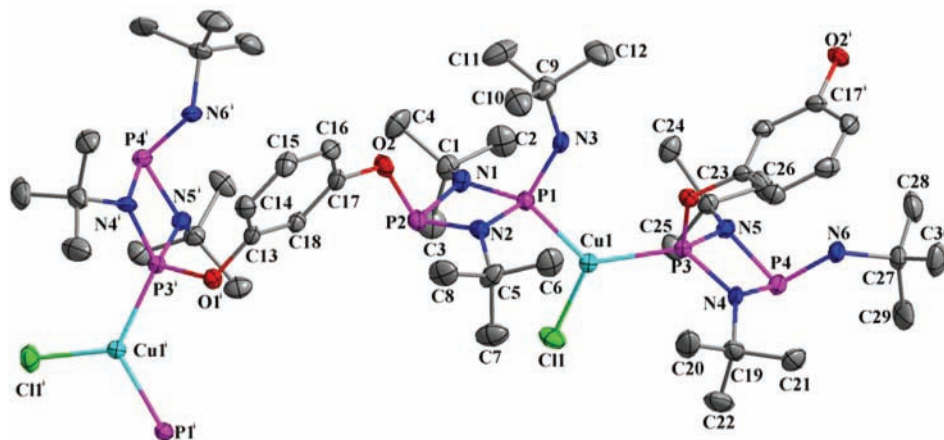


Figure 5. Molecular structure of $[\{1,3\text{-C}_6\text{H}_4(\text{OP}(\mu\text{-N}^t\text{Bu})_2\text{PN}(\text{H})^t\text{Bu})_2\}(\text{CuCl})]_n$ (7). Thermal ellipsoids are drawn at the 50% probability level. All the hydrogen atoms and lattice solvents have been omitted for clarity. Only one orientation is shown for the disordered *tert*-butyl groups.

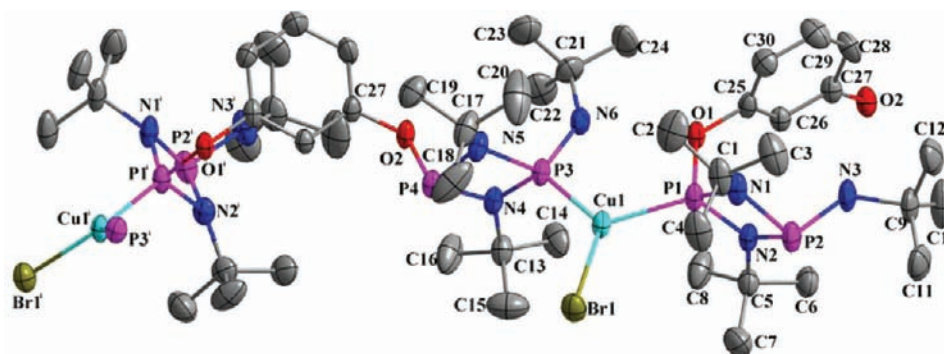


Figure 6. Molecular structure of $[\{1,3\text{-C}_6\text{H}_4(\text{OP}(\mu\text{-N}^t\text{Bu})_2\text{PN}(\text{H})^t\text{Bu})_2\}(\text{CuBr})]_n$ (8). Thermal ellipsoids are drawn at the 50% probability level. All the hydrogen atoms and lattice solvents have been omitted for clarity. Only one orientation is shown for the disordered *tert*-butyl groups. Symmetry operation (i) $-x, -y, -z$.

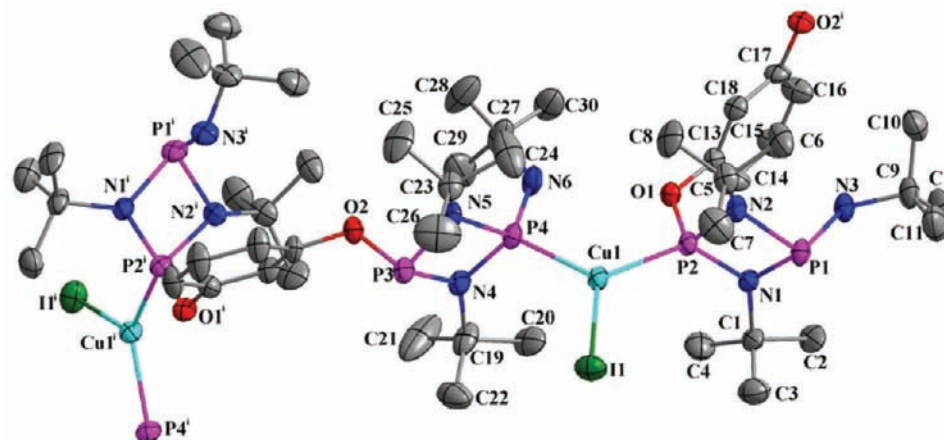


Figure 7. Molecular structure of $[\{1,3\text{-C}_6\text{H}_4(\text{OP}(\mu\text{-N}^t\text{Bu})_2\text{PN}(\text{H})^t\text{Bu})_2\}(\text{CuI})]_n$ (9). Thermal ellipsoids are drawn at the 50% probability level. All the hydrogen atoms and lattice solvents have been omitted for clarity. Only one orientation is shown for the disordered *tert*-butyl groups. Symmetry operation (i) $-x, -y, -z$.

the tetra-coordinated copper and the shorter set [2.5099(6) and 2.5790(11) Å] with the tricoordinated copper. The increase in the coordination number is responsible for the increase in the bond angle from I1–Cu1–I2 [104.03(3)°] to I1–Cu2–I2 [117.11(2)°].^{7a}

In the symmetrical $[\text{Cu}_3(\mu\text{-I}_{3,4})\text{Cu}_4]$ rhombic unit, the copper centers are tetrahedrally coordinated by one inner phosphorus, two iodine atoms, and one acetonitrile molecule.

The angles about metals are varying from 114.18(10)° for N8–Cu3–P2 to 97.06(10)° for N8–Cu3–I3. The mean planes of $[\text{Cu}_3(\mu\text{-I}_{3,4})\text{Cu}_4]$ unit are inclined at an angle of 33.18° to the plane of the aromatic ring. The Cu–I bond lengths are almost identical, with the mean distance being 2.671 Å. The Cu–I bond distances are in good agreement with the reported value for the $[\text{Cu}_2(\mu\text{-I})_2]$ unit, in $[\text{Cu}_2\text{I}_2\{\text{tBuNP}(\text{OC}_6\text{H}_4\text{OMe}-o)\}_2]_n$,^{7a} $[\text{Cu}_8(\mu\text{-I})_8(\text{CH}_3\text{CN})_4(\mu\text{-N}^t\text{BuP})_8(\text{NC}_4\text{H}_8\text{NMe})_8]$,^{6c}

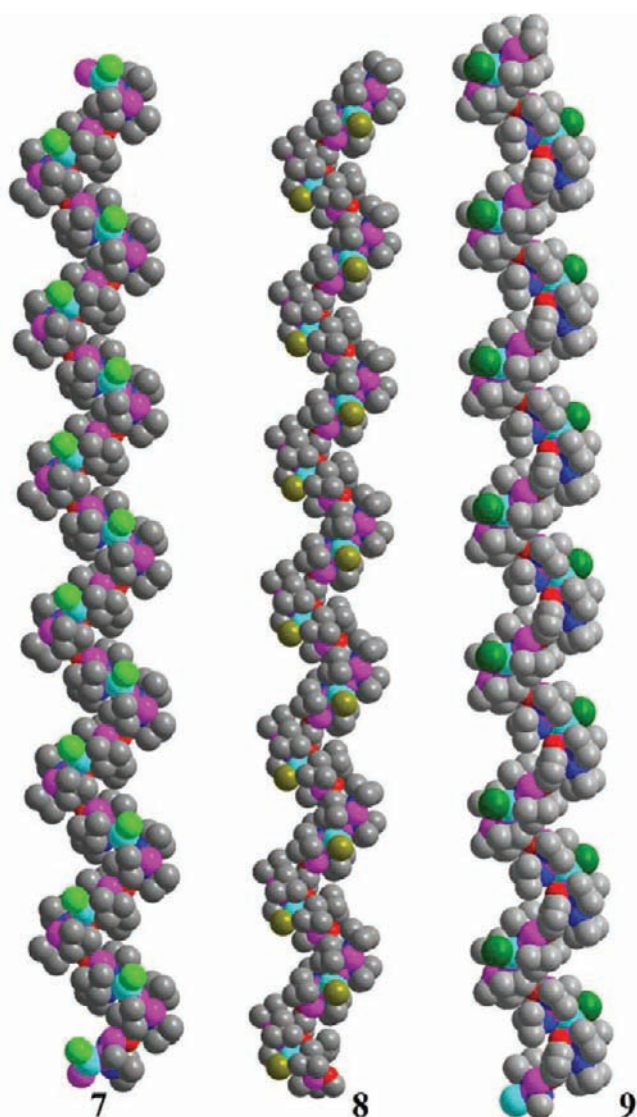


Figure 8. Helical structures of 7, 8, and 9.

and $[\text{Cu}(\mu\text{-I})(\text{dppp})]_2$.²³ Both the rhombic $[\text{Cu}_2(\mu\text{-I})_2]$ units are puckered, but the deviation from planarity is more in case of unsymmetrical $[\text{Cu1}(\mu\text{-I1,I2})\text{Cu2}]$ [$19.734(33)^\circ$] than symmetrical $[\text{Cu3}(\mu\text{-I3,I4})\text{Cu4}]$ [$9.360(16)^\circ$] unit. The $\text{Cu1}\cdots\text{Cu2}$ distance is $2.9159(7)$ Å, whereas the $\text{Cu3}\cdots\text{Cu4}$ distance is

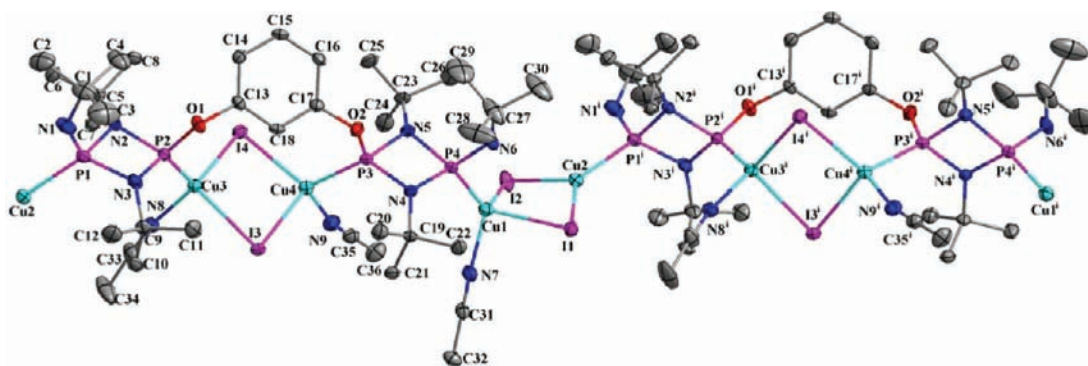


Figure 9. Molecular structure of $[\{1,3\text{-C}_6\text{H}_4(\text{OP}(\mu\text{-N}^t\text{Bu})_2\text{PN}(\text{H})^t\text{Bu})_2\}\{\text{Cu}_2(\mu\text{-I})_2\}]_n$ (**12**). Thermal ellipsoids are drawn at the 50% probability level. All the hydrogen atoms and lattice solvents have been omitted for clarity. Only one orientation is shown for the disordered *tert*-butyl groups. Symmetry operations (i) $-x, -y, -z$. (ii) $1/2-x, 1/2-y, -z$.

$3.3957(8)$ Å. This difference arises again as a result of the increase in the coordination number from three to four. In both the cases, the $\text{Cu}\cdots\text{Cu}$ distances are noticeably greater than the sum of the van der Waals radii for the copper(I) ion, which confirms the nonexistence of metallophilic interactions in coordination polymer **12**.

CONCLUSIONS

The stoichiometry controlled reactions of copper(I) halides with tetradentate ligand **1** led to the formation of 1D coordination polymers. The prediction of the structures of products in the reactions of **1** with 1 equiv of copper(I) halides were not easy, since there were four potential coordinating phosphorus centers in close proximity, but because of the steric and intramolecular hydrogen bonding, complexes **7–9** form 1D chains and adopt helical structures in solid state. The 4 equiv of copper(I) halides reacted differently with **1**, though they gave 1D coordination polymers, the propagation of polymeric chain is through the formation of rhombic $[\text{Cu}(\mu\text{-X})_2]$ units. Interestingly, in the lattice of complex **12**, the nitrogen bound *tert*-butyl groups from four neighboring units together make a hydrophobic pocket to trap two dichloromethane molecules. The dimer (**2a**) and tetramer (**2b**) were isolated from the reaction of resorcinol with $[\text{CIP}(\mu\text{-N}^t\text{Bu})]_2$. Preliminary studies have shown that the dimer can act as a tetradentate ligand. With carefully chosen transition metal precursors, these macrocycles can form polynuclear clusters and cages; some of which might mimic the properties of various synthetic zeolites. The ligand **1** with the resorcinol moiety bridging the two cyclodiphosphazane units was essentially synthesized to employ as a pincer ligand to coordinate to transition metal derivatives. It would be interesting to make pincer complexes involving inner phosphorus centers and ortho-CH activation, while the outer ones can function as either neutral or anionic ligands to form heterometallic complexes. The amide functionalities can also bind to early transition metals in their high-valent states that might result in the formation of simple dimeric to high nuclearity clusters or multinuclear 3D-coordination polymers with cavities of considerable size to trap selective organic molecules. The work in these directions is in progress.

EXPERIMENTAL SECTION

General Procedures. All manipulations were performed using standard vacuum-line and Schlenk techniques under nitrogen

Table 1. Crystallographic Information for Compounds 1, 2a, 2b, 4, 7–9, and 12

	1	2a	2b	4	7	8	9	12
formula	C ₃₀ H ₆₀ N ₆ O ₂ P ₄	C ₂₈ H ₄₄ N ₄ O ₄ P ₄	C ₅₆ H ₈₈ N ₈ O ₈ P ₈	C ₂₈ H ₄₄ N ₄ O ₄ P ₄ Se ₄	C ₂₀ H ₄₀ Cl ₈ Cu ₈ N ₈ O ₁₆ P ₃₂ ·4CH ₃ CN·2CH ₂ Cl ₂	C ₃₀ H ₆₀ B ₆ Cu ₆ N ₆ O ₂ P ₄	C ₃₀ H ₆₀ Cu ₁₀ N ₆ O ₂ P ₄	C ₃₀ H ₆₀ Cu ₄ I ₄ N ₆ O ₂ P ₄ ·0.24CH ₂ Cl ₂ ·CH ₃ CN
FW	660.72	624.55	1249.10	940.39	6411.83	804.17	851.16	1607.93
crystal system	monoclinic	monoclinic	monoclinic	monoclinic	orthorhombic	monoclinic	orthorhombic	monoclinic
space group	C2/c	P21/n	P21/n	P21/c	Pna21	P21/n	Pbca	C2/c
a, Å	26.304(9)	18.0803(18)	14.0072(15)	12.0127(6)	19.742(2)	10.8133(10)	19.993(4)	38.942(5)
b, Å	9.647(3)	10.1715(10)	9.5032(10)	13.9234(7)	13.3563(16)	26.476(2)	18.277(4)	11.0604(13)
c, Å	15.030(5)	18.0946(18)	25.390(3)	11.9517(6)	33.573(4)	16.7607(15)	22.778(4)	32.778(4)
α, deg	90	90	90	90	90	90	90	90
β, deg	98.622(5)	103.199(1)	97.656(2)	110.451(1)	90	90.645(1)	90	119.582(1)
γ, deg	90	90	90	90	90	90	90	90
V, Å ³	3771(2)	3239.8(6)	3349.6(6)	1873.02(16)	8852.5(17)	4798.2(7)	8323(3)	12278(3)
Z	4	4	2	2	1	4	8	8
ρ _{calc} , g cm ⁻³	1.164	1.281	1.238	1.667	1.203	1.113	1.359	1.740
μ(Mo Kα), mm ⁻¹	0.234	0.271	0.262	4.126	0.762	1.449	1.453	3.542
F(000)	1432	1328	1328	936	3404	1688	3520	6276
T (K)	100	195	100	100	100	100	100	100
2θ range, deg	2.3–28.1	2.0–28.8	2.3–28.4	2.3–28.8	1.2–27.5	1.4–27.2	1.8–26.5	1.4–28.0
total no. of reflns	31880	56836	55995	32446	74797	78026	64232	52953
no. of indep. reflns	4575 [R _{int} = 0.064]	8368 [R _{int} = 0.057]	8368 [R _{int} = 0.045]	4802 [R _{int} = 0.034]	20067 [R _{int} = 0.092]	10620 [R _{int} = 0.058]	8607 [R _{int} = 0.116]	14523 [R _{int} = 0.028]
R ^a	0.0376	0.0668	0.0380	0.0217	0.0569	0.0434	0.0590	0.0277
wR ^a	0.0994	0.2083	0.0982	0.0560	0.1289	0.1153	0.1742	0.0652
S	1.04	1.05	1.03	1.06	0.95	1.03	1.02	1.05

$$a_w = 1/[\sigma^2(F_o^2) + (0.0318P)^2 + 0.7734P] \text{ where } P = (F_o^2 + 2F_c^2)/3.$$

Table 2. Selected Bond Distances (Å) and Bond Angles (deg) for 1, 2a, 2b, and 4

compound 1				compound 2a			
bond length (Å)		bond angle (deg)		bond length (Å)		bond angle (deg)	
P1–O1	1.6705(13)	O1–P1–N1	104.56(6)	P1–O1	1.662(3)	N1–P1–N2	81.28(18)
P1–N1	1.6990(14)	O1–P1–N2	104.85(6)	P1–N1	1.709(4)	O1–P1–N1	105.32(17)
P1–N2	1.6941(14)	N1–P1–N2	82.37(6)	P1–N2	1.706(4)	O1–P1–N2	99.15(16)
P2–N1	1.7362(14)	N1–P2–N2	79.98(6)	P2–O2	1.647(3)	P1–N1–P2	97.8(2)
P2–N2	1.7406(14)	N1–P2–N3	103.52(7)	P2–N1	1.706(4)	O2–P2–N1	109.94(19)
P2–N3	1.6480(15)	N2–P2–N3	105.31(7)	P2–N2	1.715(4)	O3–P3–N3	98.84(15)
O1–C1	1.384(2)	P1–N1–P2	98.25(7)	P4–O4	1.653(3)	N3–P4–N4	80.37(18)
						O4–P4–N4	110.47(17)
						P3–N4–P4	97.88(19)
compound 2b				compound 4			
bond length (Å)		bond angle (deg)		bond length (Å)		bond angle (deg)	
P1–N1	1.7000(14)	N1–P1–N2	81.77(7)	Se1–P1	2.0670(4)	N1–P2–N2	83.95(6)
P1–N2	1.7091(14)	O4–P1–N1	100.54(6)	Se2–P2	2.0631(4)	O1–P1–N1	103.25(6)
P1–O4	1.6598(13)	O1–P2–N2	105.72(6)	P1–O1	1.5981(11)	O1–P1–N2	106.01(6)
P2–O1	1.6614(12)	O2–P3–N3	103.78(6)	P1–N1	1.6816(14)	P1–N1–P2	95.10(6)
P3–O2	1.6673(12)	N3–P3–N4	80.88(7)	P1–N2	1.6832(13)	O2–P2–N1	110.24(6)
P4–O3	1.6551(15)	O3–P4–N3	107.48(7)	P2–O2	1.6039(11)	O2–P2–N2	110.63(6)
						Se1–P1–P2	128.04(2)
						Se1–P1–O1	115.22(4)
						Se1–P1–N1	120.84(4)

Table 3. Selected Bond Distances (Å) and Bond Angles (deg) for 7, 8, 9, and 12

compound 7				compound 8			
bond length (Å)		bond angle (deg)		bond length (Å)		bond angle (deg)	
Cu1–P3	2.2101(14)	P1–Cu1–P3	119.30(5)	Cu–Br1	2.3454(5)	Br1–Cu1–P1	117.48(3)
Cu1–Cl1	2.1970(14)	Cl1–Cu1–P1	117.80(5)	Cu1–P1	2.2431(9)	Br1–Cu1–P3a	124.26(3)
Cu1–P1	2.2300(14)	Cl1–Cu1–P3	122.88(5)	Cu1–P3	2.2516(9)	P1–Cu1–P3a	118.24(3)
P1–N2	1.712(4)	Cu1–P1–N2	115.38(15)	P1–O1	1.660(2)	Cu1–P1–O1	104.14(7)
P1–N1	1.703(4)	Cu1–P1–N3	109.61(15)	P1–N1	1.672(2)	Cu1–P1–N1	130.83(9)
P1–N3	1.647(4)	N2–P1–N3	114.0(2)	P1–N2	1.677(2)	Cu1–P1–N2	122.14(9)
P2–O2	1.673(4)	Cu1–P3–N5	122.25(15)	P2–N1	1.746(2)	N1–P1–N2	84.30(12)
P3–O1	1.668(3)	Cu1–P3–O1	105.38(11)	P3–N4	1.719(2)	N1–P2–N2	79.71(11)
		Cu1–P3–N4	129.65(14)	P4–O2	1.673(2)	N1–P2–N3	104.61(13)
compound 9				compound 12			
bond length (Å)		bond angle (deg)		bond length (Å)		bond angle (deg)	
Cu1–I1	2.4878(9)	I1–Cu1–P2	120.75(5)	I1–Cu1	2.8168(6)	Cu1–I1–Cu2	66.09(1)
Cu1–P2	2.2279(16)	I1–Cu1–P4	119.07(4)	I1–Cu2	2.5099(6)	Cu1–I2–Cu2	67.15(2)
Cu1–P4	2.2518(16)	P2–Cu1–P4	120.13(6)	I2–Cu1	2.6910(8)	Cu3–I3–Cu4	79.06(2)
P1–N1	1.755(4)	N1–P1–N2	79.40(19)	I2–Cu2	2.5790(11)	Cu3–I4–Cu4	78.79(1)
P1–N2	1.756(4)	N1–P1–N3	103.7(2)	I3–Cu3	2.6681(6)	I1–Cu1–I2	104.03(3)
P1–N3	1.651(4)	N2–P1–N3	105.7(2)	I3–Cu4	2.6668(6)	I1–Cu1–N7	96.15(10)
P2–O1	1.659(4)	Cu1–P2–O1	103.48(14)	I4–Cu3	2.6798(6)	I4–Cu4–P3	118.66(3)
P2–N1	1.670(4)	Cu1–P2–N1	130.02(16)	Cu1–N7	1.999(3)	I1–Cu2–P1	128.19(3)
P3–O2	1.678(4)	Cu1–P2–N2	124.09(15)	Cu1–P4	2.2291(11)	I2–Cu2–P1	114.54(3)
		O1–P2–N1	105.9(2)	Cu2–P1	2.2151(10)	I3–Cu3–I4	100.19(2)
				Cu3–P2	2.2077(10)	I3–Cu3–N8	97.06(10)
				Cu3–N8	2.040(3)	I4–Cu3–P2	117.59(3)
				Cu4–P3	2.2149(10)	I3–Cu4–I4	100.45(2)
				Cu4–N9	2.053(4)	I3–Cu4–N9	103.97(9)

atmosphere unless otherwise stated. All of the solvents were purified by conventional procedures²⁴ and distilled prior to use. The compounds *cis*-[^tBuHN(^tBuNP)₂Cl]₂,²⁵ *cis*-[ClP(μ -N^tBu)]₂,²⁵ AuCl(SMe₂),²⁶ [Pd(η^3 -C₃H₅)Cl]₂,²⁷ CuCl,²⁸ and CuBr²⁸ were prepared according to the published procedures. CuI was purchased from Aldrich chemicals and used as such without further purification. Other chemicals were obtained from commercial sources and purified prior to use.

Instrumentation. The NMR spectra were recorded at the following frequencies: 400 MHz (¹H), 100 MHz (¹³C), 162 MHz (³¹P) using either Varian VXR 400 or Bruker AV 400 spectrometers. ¹³C and ³¹P NMR spectra were acquired using broad band decoupling. The spectra were recorded in CDCl₃ (or DMSO-d₆) solutions with CDCl₃ (or DMSO-d₆) as an internal lock; chemical shifts of ¹H and ¹³C NMR spectra are reported in ppm downfield from TMS, used as internal standard. The chemical shifts of ³¹P NMR spectra are referred

to 85% H₃PO₄ as external standard. The microanalyses were performed using a Carlo Erba Model 1112 elemental analyzer. Mass spectra were recorded using Waters Q-ToF micro (YA-105). The melting points were observed in capillary tubes and are uncorrected.

Synthesis of [1,3-C₆H₄(OP(μ-NⁱBu)₂PN(H)ⁱBu)₂]₂ (1). A mixture of resorcinol (0.375 g, 3.4 mmol) and triethylamine (0.84 g, 1.2 mL, 8.3 mmol) in diethyl ether (25 mL) was added dropwise to an ice cold solution of *cis*-[CIP(μ-NⁱBu)₂PN(H)ⁱBu] (2.14 g, 6.8 mmol) also in diethyl ether (25 mL). After the completion of the addition, the reaction mixture was stirred for 12 h at room temperature and then filtered through Celite to remove amine hydrochloride salt. Solvent was removed under reduced pressure to obtain **1** as a white solid, which was then recrystallized from toluene. Yield: 89% (2.0 g). Mp: 94–96 °C. Anal. Calcd for C₃₀H₆₀N₆O₂P₄: C, 54.53; H, 9.15; N, 12.72. Found: C, 54.17; H, 9.19; N, 12.65. ¹H NMR (400 MHz, CDCl₃): δ 7.19 (t, ³J_{HH} = 8 Hz, ArH, 1H), 6.80–6.83 (m, ArH, 3H), 2.42 (d, NH, ²J_{PH} = 8 Hz, 2H), 1.34 (s, ⁱBu, 36H), 1.12 (s, ⁱBu, 18H). ¹³C{¹H} NMR (100 MHz, CDCl₃): 153.5, 127.9, 118.1, 117.9, 52.2 (vt, ²J_{PC} = 13.1 Hz), 51.5 (d, ²J_{PC} = 14.1 Hz), 32.9 (d, ³J_{PC} = 9.2 Hz), 31.5 (vt, ³J_{PC} = 6.3 Hz). ³¹P{¹H} NMR (162 MHz, CDCl₃): δ 129.7 (s), 100.1 (s). MS (EI): *m/z* = 661.1 (M+1).

Synthesis of [P(μ-NⁱBu)₂{1,3-(O)₂-C₆H₄}]₂ (2a) and [P(μ-NⁱBu)₂{1,3-(O)₂-C₆H₄}]₄ (2b). A mixture of resorcinol (1.2 g, 10.9 mmol) and triethylamine (2.77 g, 3.9 mL, 27.42 mmol) in diethyl ether (50 mL) was added dropwise to an ice-cold solution of *cis*-[CIP(μ-NⁱBu)₂]₂ (3.0 g, 10.9 mmol) also in diethyl ether (30 mL). After the completion of the addition, the reaction mixture was stirred for 12 h at room temperature and then filtered through Celite to remove amine hydrochloride salt. Solvent was removed under vacuum to obtain product as a white solid. The crude mixture was passed through a silica gel column using 9:1 mixture of pet-ether and dichloromethane as eluent, and both fractions were recrystallized from toluene.

Yield (2a): 26% (0.9 g). Mp: 106–108 °C. Anal. Calcd for C₆H₈N₈O₈P₈: C, 53.85; H, 7.10; N, 8.97. Found: C, 53.77; H, 7.11; N, 9.02. ¹H NMR (400 MHz, CDCl₃): δ 8.39 (s, ArH, 2H), 7.12 (t, ³J_{HH} = 8 Hz, ArH, 2H), 6.74 (d, ³J_{HH} = 8 Hz, ArH, 4H), 1.27 (s, ⁱBu, 36H). ³¹P{¹H} NMR (162 MHz, CDCl₃): δ 131.5 (s). MS (EI): *m/z* = 625.2 (M+1⁺).

Yield (2b): 20% (0.7 g). Mp: 120–124 °C. Anal. Calcd for C₆H₈N₈O₈P₈: C, 53.85; H, 7.10; N, 8.97. Found: C, 53.69; H, 6.97; N, 8.83. ¹H NMR (400 MHz, CDCl₃): δ 7.17 (t, ³J_{HH} = 8 Hz, ArH, 4H), 6.85–6.94 (m, ArH, 12H), 1.35 (s, ⁱBu, 36H). ³¹P{¹H} NMR (162 MHz, CDCl₃): δ 146.0 (s).

Synthesis of [O=P(μ-NⁱBu)₂{1,3-(O)₂-C₆H₄}]₂ (3). A 30% aqueous solution of H₂O₂ (0.007 g, 0.021 mL, 0.206 mmol) in THF (5 mL) was added dropwise to a well-stirred THF solution (10 mL) of **2a** (0.03 g, 0.048 mmol). The reaction mixture was stirred for 5 h at room temperature. The solvent was removed under reduced pressure to give **3** as off-white solid. Yield: 85% (0.028 g). Mp: 168–172 °C. HRMS Calc for C₂₈H₄₅N₄O₄P₄: 689.2188, Found: 689.2172. ¹H NMR (400 MHz, CDCl₃): δ 7.83 (t, ³J_{HH} = 2.4 Hz ArH, 2H), 7.42–7.36 (m, ArH, 6H), 1.39 (s, ⁱBu, 36H). ³¹P{¹H} NMR (162 MHz, CDCl₃): –11.9 (s). MS (EI): *m/z* = 689.2 (M+1).

Synthesis of [Se=P(μ-NⁱBu)₂{1,3-(O)₂-C₆H₄}]₂ (4). A mixture of [P(μ-NⁱBu)₂{1,3-(O)₂-C₆H₄}]₂ (**2a**) (0.04 g, 0.064 mmol) and selenium (0.021 g, 0.266 mmol) in 20 mL of toluene was refluxed for 24 h. Then the solution was cooled to room temperature and filtered through Celite, and the solvent was removed under reduced pressure to get compound **4** as a yellow crystalline solid. Yield: 89% (0.054 g). Mp: >270 °C. Anal. Calcd for C₂₈H₄₄N₄O₄P₄Se₄: C, 35.76; H, 4.72; N, 5.96. Found: C, 35.67; H, 4.65; N, 5.90. ¹H NMR (400 MHz, CDCl₃): δ 7.83 (s, ArH, 2H), 7.36 (t, ³J_{HH} = 8 Hz, ArH, 2H), 7.24 (d, ³J_{HH} = 8 Hz, ArH, 4H), 1.60 (s, ⁱBu, 36H). ³¹P{¹H} NMR (162 MHz, CDCl₃): 32.7 (s, ¹J_{PSe} = 996 Hz, ²J_{PP} = 7.3 Hz). MS (EI): *m/z* = 940.3 (M+1).

Synthesis of [(Cl)(η³-C₃H₅)PdP(μ-NⁱBu)₂{1,3-(O)₂-C₆H₄}]₂ (5). A dichloromethane solution (10 mL) of [Pd(μ-Cl)(η³-C₃H₅)₂] (0.0316 mg, 0.0864 mmol) was added to [P(μ-NⁱBu)₂{1,3-(O)₂-C₆H₄}]₂ (**2a**) (0.027 g, 0.0432 mmol) in 10 mL of dichloromethane at room temperature. The resultant turbid solution was stirred under

reflux for 10 h. The solvent was removed under reduced pressure, to get **5** as an off-white solid. Yield: 75% (0.044 g). Mp: >210 °C (dec). Anal. Calcd for C₄₀H₆₄Cl₄N₄O₄P₄Pd₄: C, 35.42; H, 4.76; N, 4.13. Found: C, 35.31; H, 4.92; N, 4.09. ¹H NMR (400 MHz, CDCl₃): δ 7.83 (s, ArH, 2H), 7.40–6.81 (m, br, ArH, 6H), 5.74–5.30 (m, br, CH₂, 4H), 4.76 (m, CH₂, 6H), 3.76 (m, CH₂, 6H), 3.19 (t, *J* = 14.6 Hz, CH₂, 4H), 1.57–1.43 (m, ⁱBu, 36H). ³¹P{¹H} NMR (162 MHz, CDCl₃): δ 122.7 (br, s), 115.0 (br, s).

Synthesis of [(ClAu)P(μ-NⁱBu)₂{1,3-(O)₂-C₆H₄}]₂ (6). A dichloromethane (10 mL) solution of AuCl(SMe₂) (0.047 g, 0.16 mmol) was added dropwise over a well-stirred solution (10 mL) of [P(μ-NⁱBu)₂{1,3-(O)₂-C₆H₄}]₂ (**2a**) (0.025 g, 0.04 mmol) at room temperature. The reaction mixture was stirred further for 5 h under minimum exposure of light, and then solvent was removed under vacuum, washed with 2 × 5 mL of pet ether, to get an analytically pure white solid. Yield: 81% (0.049 g). Mp: >270 °C (dec). Anal. Calcd for C₂₈H₄₄Au₄Cl₄N₄O₄P₄: C, 21.64; H, 2.85; N, 3.60. Found: C, 21.56; H, 2.83; N, 3.46. ¹H NMR (400 MHz, CDCl₃): δ 7.89 (s, ArH, 2H), 7.43 (s, br, ArH, 2H), 7.24 (s, br, ArH, 4H), 1.57 (s, ⁱBu, 36H). ³¹P{¹H} NMR (162 MHz, CDCl₃): δ 98.4 (s).

Synthesis of [1,3-C₆H₄(OP(μ-NⁱBu)₂PN(H)ⁱBu)₂](CuCl)_n (7). A solution of cuprous chloride (0.0066 g, 0.0666 mmol) in acetonitrile (5 mL) was added dropwise to a solution of **1** (0.044 g, 0.0666 mmol) also in dichloromethane (5 mL). The reaction mixture was allowed to stir at room temperature for 4 h. The resulting white precipitate was washed with 5 mL of petroleum ether, to get analytical pure **7** as white powder. Yield: 85% (0.043 g). Mp: 155–158 °C. Anal. Calcd for C_{31.25}H₆₂Cl_{1.5}Cu_{N_{6.5}O₂P₄}: C, 46.83; H, 7.80; N, 11.36. Found: C, 46.79; H, 7.72; N, 11.27. ¹H NMR (400 MHz, CDCl₃): δ 7.10–6.50 (m, ArH, 4H), 4.67 (br, s, NH, 2H), 1.57 (s, ⁱBu, 36H), 1.38 (s, ⁱBu, 18H). ³¹P{¹H} NMR (162 MHz, CDCl₃): δ 135.6 (br, s), 98.7 (br, s), 73.8 (br, s), 67.2 (br, s).

Synthesis of [1,3-C₆H₄(OP(μ-NⁱBu)₂PN(H)ⁱBu)₂](CuBr)_n (8). Compound **8** was synthesized by a procedure similar to that of **7** using cuprous bromide (0.0062 g, 0.0216 mmol) and **1** (0.029 g, 0.0216 mmol). Yield: 82% (0.029 g). Mp: 200–202 °C. Anal. Calcd for C₃₀H₆₀CuBrN₆O₂P₄: C, 44.80; H, 7.52; N, 10.45. Found: C, 44.78; H, 7.39; N, 10.34. ¹H NMR (400 MHz, DMSO-*d*₆): δ 7.30–6.61 (m, ArH, 4H), 4.70 (br, s, NH, 2H), 1.41–1.30 (m, ⁱBu, 54H). ³¹P{¹H} NMR (162 MHz, DMSO-*d*₆): δ 139.4 (br, s), 101.3 (br, s), 71.4 (br, s).

Synthesis of [1,3-C₆H₄(OP(μ-NⁱBu)₂PN(H)ⁱBu)₂](CuI)_n (9). Compound **9** was synthesized by a procedure similar to that of **7** using cuprous iodide (0.0104 g, 0.0546 mmol) and **1** (0.036 g, 0.0546 mmol). Yield: 84% (0.039 g). Mp: 175–178 °C. Anal. Calcd for C₃₀H₆₀CuIN₆O₂P₄: C, 42.33; H, 7.10; N, 9.87. Found: C, 42.16; H, 6.95; N, 9.69. ¹H NMR (400 MHz, DMSO-*d*₆): δ 7.65 (m, ArH, 4H), 4.89 (br, s, NH, 2H), 1.43–1.23 (m, ⁱBu, 54H). ³¹P{¹H} NMR (162 MHz, DMSO-*d*₆): δ 134.5 (br, s), 97.6 (br, s), 72.3 (br, s), 67.9 (br, s).

Synthesis of [1,3-C₆H₄(OP(μ-NⁱBu)₂PN(H)ⁱBu)₂](Cu₂(μ-Cl)₂)_n (10). Compound **10** was synthesized by a procedure similar to that of **7** using cuprous chloride (0.018 g, 0.182 mmol) and **1** (0.03 g, 0.0454 mmol). Yield: 85% (0.041 g). Mp: 219–222 °C. Anal. Calcd for C₃₆H₆₉Cu₄Cl₄N₉O₂P₄2CH₂Cl₂: C, 33.81; H, 5.45; N, 9.33. Found: C, 33.63; H, 5.37; N, 9.25. ¹H NMR (400 MHz, DMSO-*d*₆): δ 7.80–6.85 (m, ArH, 4H), 4.85 (br, s, NH, 2H), 1.57–1.30 (m, ⁱBu, 54H). ³¹P{¹H} NMR (162 MHz, DMSO-*d*₆): δ 107.9 (br, s), 80.0 (br, s), 66.5 (br, s).

Synthesis of [1,3-C₆H₄(OP(μ-NⁱBu)₂PN(H)ⁱBu)₂](Cu₂(μ-Br)₂)_n (11). Compound **11** was synthesized by a procedure similar to that of **7** using cuprous bromide (0.016 g, 0.112 mmol) and **1** (0.0184 g, 0.0278 mmol). Yield: 78% (0.027 g). Mp: >270 °C (dec). Anal. Calcd for C₃₆H₆₉Cu₄Br₄N₉O₂P₄: C, 31.85; H, 5.12; N, 9.28. Found: C, 31.87; H, 5.25; N, 8.65. ¹H NMR (400 MHz, DMSO-*d*₆): δ 7.30–6.60 (m, ArH, 4H), 4.70 (br, s, NH, 2H), 1.52 (s, ⁱBu, 36H), 1.35 (s, ⁱBu, 18H). ³¹P{¹H} NMR (162 MHz, DMSO-*d*₆): δ 106.5 (br, s), 78.6 (br, s), 66.2 (br, s).

Synthesis of [1,3-C₆H₄(OP(μ-NⁱBu)₂PN(H)ⁱBu)₂](Cu₂(μ-I)₂)_n (12). Compound **12** was synthesized by a procedure similar to that of **7** using cuprous iodide (0.106 g, 0.559 mmol) and **1** (0.092 g, 0.139

mmol. Yield: 86% (0.171 g). Mp: 236–240 °C. Anal. Calcd for $C_{36}H_{69}Cu_4I_4N_9O_2P_4$: C, 27.97; H, 4.49; N, 8.15. Found: C, 27.62; H, 4.34; N, 8.01. 1H NMR (400 MHz, DMSO- d_6): δ 7.36 (t, $^3J_{HH} = 7.2$ Hz, ArH, 1H), 7.16 (br, s, ArH, 1H), 6.85 (br, s, ArH, 2H), 4.85 (br, s, NH, 1H), 4.46 (br, s, NH, 1H), 1.50 (s, tBu , 36H), 1.38 (s, tBu , 18H). $^{31}P\{^1H\}$ NMR (162 MHz, DMSO- d_6): δ 106.5 (br, s), 79.0 (br, s), 67.3 (br, s).

X-ray Crystallography. Crystals of each of the compounds **1**, **2a**, **2b**, **4**, **7–9**, and **12** suitable for X-ray crystal analysis were mounted on a Cryolooop with a drop of Paratone oil and placed in the cold nitrogen stream of the Kryoflex attachment of the Bruker APEX CCD diffractometer. A full sphere of data was collected using 606 scans in ω (0.3° per scan) at $\varphi = 0$, 120 , and 240° using the SMART²⁹ software package, or the APEX2³⁰ program suite. The raw data were reduced to F^2 values using the SAINT+ software,³¹ and a global refinement of unit cell parameters using about 4575–20067 reflections chosen from the full data set were performed. Multiple measurements of equivalent reflections provided the basis for an empirical absorption correction as well as a correction for any crystal deterioration during the data collection (SADABS³²). The structures **1**, **2a**, **2b**, **4**, **7–9**, and **12** were solved by the Patterson method, while the remaining structures were solved by direct methods and refined by full-matrix least-squares procedures using the SHELXTL program package.³³ Multiple measurements of equivalent reflections provided the basis for empirical absorption corrections as well as corrections for any crystal deterioration during the data collection (SADABS). The structures were solved by direct methods or the positions of the heavy atoms were obtained from a sharpened Patterson function. Hydrogen atoms attached to carbon were placed in calculated positions and included as riding contributions with isotropic displacement parameters tied to those of the attached non-hydrogen atoms. Those attached to nitrogen were placed in locations derived from a difference map and also included as riding contributions as for the others. The isotropic thermal parameters of the hydrogen atoms were fixed at 1.2 times that of the corresponding carbon for phenyl hydrogen and 1.5 times for $C(CH_3)_3$. In the final refinement, the hydrogen atoms were riding with the carbon atom to which they were bonded.

In the structures of **8**, **9**, and **12**, the *tert*-butyl groups on exocyclic nitrogen and bridged iodine in **12** were disordered with the atoms statistically distributed over the two atomic positions. In all these structures, the two atoms were not constrained to locate in the same position, but the anisotropic thermal parameters were restricted to be equal. The details of X-ray structural determinations are given in Tables 1.

■ ASSOCIATED CONTENT

📄 Supporting Information

X-ray crystallographic files in CIF format for the structure determinations of **1**, **2a**, **2b**, **4**, **7–9**, and **12**; further details are given in Chart S1 and structures showing hydrogen bonding. This material is available free of charge via the Internet at <http://pubs.acs.org>.

■ AUTHOR INFORMATION

Corresponding Author

*E-mail: krishna@chem.iitb.ac.in or msb_krishna@iitb.ac.in. Fax: +91-22-5172-3480/2576-7152.

Notes

The authors declare no competing financial interest.

■ ACKNOWLEDGMENTS

We are grateful to the Department of Science and Technology (DST), New Delhi, for financial support of this work through Grant SR/S1/IC-17/2010. G.S.A. thanks CSIR, New Delhi, for a Research Fellowship (JRF & SRF). We also thank the Department of Chemistry Instrumentation Facilities, IIT Bombay, for spectral and analytical data and J.T.M. thanks

the Louisiana Board of Regents for the purchase of the CCD diffractometer and the Chemistry Department of Tulane University for support of the X-ray laboratory.

■ REFERENCES

- (1) (a) Balakrishna, M. S.; Eisler, D. J.; Chivers, T. *Chem. Soc. Rev.* **2007**, *36*, 650–664. (b) Briand, G. G.; Chivers, T.; Krahn, M. *Coord. Chem. Rev.* **2002**, *233/234*, 237–254. (c) Stahl, L. *Coord. Chem. Rev.* **2000**, *210*, 203–250. (d) Balakrishna, M. S.; Reddy, V. S.; Krishnamurthy, S. S.; Nixon, J. F.; Laurent, J. C. T. R. B. S. *Coord. Chem. Rev.* **1994**, *129*, 1–90.
- (2) (a) Garcia, F.; Kowenicki, R. A.; Kuzu, I.; Riera, L.; McPartlin, M.; Wright, D. S. *Dalton Trans.* **2004**, 2904–2909. (b) Chakravarty, M.; Kommana, P.; Kumara Swamy, K. C. *Chem. Commun.* **2005**, 5396–5398. (c) Dodds, F.; Garcia, F.; Kowenicki, R. A.; McPartlin, M.; Steiner, A.; Wright, D. S. *Chem. Commun.* **2005**, 3733–3735. (d) Balakrishna, M. S.; Mague, J. T. *Organometallics* **2007**, *26*, 4677–4679. (e) Kommana, P.; Kumara Swamy, K. C. *Inorg. Chem.* **2000**, *39*, 4384–4385.
- (3) Kumar, S. N.; Kumar, P. K.; Kumar, P. K. V. P.; Kommana, P.; Vittal, J. J.; Kumara Swamy, K. C. *J. Org. Chem.* **2004**, *69*, 1880–1889.
- (4) Balakrishna, M. S.; Suresh, D.; Mague, J. T. *Inorg. Chim. Acta* **2011**, *372*, 259–265.
- (5) (a) Balakrishna, M. S.; Suresh, D.; Rai, A.; Mague, J. T.; Panda, D. *Inorg. Chem.* **2010**, *49*, 8790–8801. (b) Suresh, D.; Balakrishna, M. S.; Rathinasamy, K.; Panda, D.; Mobin, S. M. *Dalton Trans.* **2008**, 2812–2814.
- (6) (a) Chandrasekaran, P.; Mague, J. T.; Balakrishna, M. S. *Dalton Trans.* **2009**, 5478–5486. (b) Chandrasekaran, P.; Mague, J. T.; Balakrishna, M. S. *Organometallics* **2005**, *24*, 3780–3783. (c) Suresh, D.; Balakrishna, M. S.; Mague, J. T. *Dalton Trans.* **2008**, 3272–3274.
- (7) (a) Chandrasekaran, P.; Mague, J. T.; Balakrishna, M. S. *Inorg. Chem.* **2006**, *45*, 6678–6683. (b) Chandrasekaran, P.; Mague, J. T.; Balakrishna, M. S. *Dalton Trans.* **2007**, 2957–2962.
- (8) (a) Alyea, E. C.; Ferguson, G.; Malito, J.; Ruhl, B. L. *Inorg. Chem.* **1985**, *24*, 3719–3720. (b) Barron, P. F.; Dyason, J. C.; Healy, P. C.; Engelhardt, L. M.; Pakawatchai, C.; Patrick, V. A.; White, A. H. *J. Chem. Soc., Dalton Trans.* **1987**, 1099–1106. (c) Graham, P. M.; Pike, R. D.; Sabat, M.; Bailey, R. D.; Pennington, W. T. *Inorg. Chem.* **2000**, *39*, 5121–5132. (d) Churchill, M. R.; Rotella, R. J. *Inorg. Chem.* **1979**, *18*, 166–171.
- (9) (a) Barron, P. F.; Dyason, J. C.; Engelhardt, L. M.; Healy, P. C.; White, A. H. *Inorg. Chem.* **1984**, *23*, 3766–3769. (b) Ganesamoorthy, C.; Mague, J. T.; Balakrishna, M. S. *Eur. J. Inorg. Chem.* **2008**, 596–604.
- (10) (a) Ganesamoorthy, C.; Balakrishna, M. S.; George, P. P.; Mague, J. T. *Inorg. Chem.* **2007**, *47*, 848–858. (b) Fu, W.-F.; Gan, X.; Che, C.-M.; Cao, Q.-Y.; Zhou, Z.-Y.; Zhu, N. N.-Y. *Chem.—Eur. J.* **2004**, *10*, 2228–2236. (c) Araki, H.; Tsuge, K.; Sasaki, Y.; Ishizaka, S.; Kitamura, N. *Inorg. Chem.* **2005**, *44*, 9667–9675.
- (11) (a) Liu, Z.; Djurovich, P. I.; Whited, M. T.; Thompson, M. E. *Inorg. Chem.* **2012**, *51*, 230–236. (b) Zink, D. M.; Grab, T.; Baumann, T.; Nieger, M.; Barnes, E. C.; Klopffer, W.; Brase, S. *Organometallics* **2011**, *30*, 3275–3283. (c) Chakrabarty, R.; Mukherjee, P. S.; Stang, P. J. *Chem. Rev.* **2011**, *111*, 6810–6918.
- (12) (a) Balakrishna, M. S. *J. Organomet. Chem.* **2010**, *695*, 925–936. (b) Balakrishna, M. S.; Chandrasekaran, P.; Venkateswaran, R. J. *Organomet. Chem.* **2007**, *692*, 2642–2648.
- (13) Balakrishna, M. S.; Venkateswaran, R.; Mague, J. T. *Inorg. Chem.* **2009**, *48*, 1398–1406.
- (14) (a) Vijjulatha, M.; Kumaraswamy, S.; Kumara Swamy, K. C.; Engelhardt, U. *Polyhedron* **1999**, *18*, 2557–2562. (b) Kumaravel, S. S.; Krishnamurthy, S. S.; Cameron, T. S.; Linden, A. *Inorg. Chem.* **1988**, *27*, 4546–4550. (c) Garcia, F.; Goodman, J. M.; Kowenicki, R. A.; McPartlin, M.; Riera, L.; Silva, M. I. A.; Wirsing, A.; Wright, D. S. *Dalton Trans.* **2005**, 1764–1773. (d) Calera, S. G.; Wright, D. S. *Dalton Trans.* **2010**, *39*, 5055–5065.

- (15) Chandrasekaran, P.; Mague, J. T.; Balakrishna, M. S. *Inorg. Chem.* **2006**, *45*, 5893–5897.
- (16) Colquhoun, I. J.; Christina, H.; McFarlane, E.; McFarlane, W.; Nash, J. A.; Keat, R.; Rycroft, D. S.; Thompson, D. G. *Org. Magn. Reson.* **1979**, *12*, 473–475.
- (17) (a) Lief, G. R.; Moser, D. F.; Stahl, L.; Staples, R. J. *J. Organomet. Chem.* **2004**, *689*, 1110–1121. (b) Suresh, D.; Balakrishna, M. S.; Mague, J. T. *2007*, *48*, 2283–2285.
- (18) Balakrishna, M. S.; Venkateswaran, R.; Mague, J. T. *Dalton Trans.* **2010**, *39*, 11149–11162.
- (19) Calera, S. G.; Eisler, D. J.; Goodman, J. M.; McPartlin, M.; Singh, S.; Wright, D. S. *Dalton Trans.* **2009**, 1293–1296.
- (20) Bowmaker, G. A.; Boyd, S. E.; Hanna, J. V.; Hart, R. D.; Healy, P. C.; Skelton, B. W.; White, A. H. *J. Chem. Soc., Dalton Trans.* **2002**, 2722–2730.
- (21) Bowmaker, G. A.; Dyason, J. C.; Healy, P. C.; Engelhardt, L. M.; Pakawatchai, C.; White, A. H. *J. Chem. Soc., Dalton Trans.* **1987**, 1089–1097.
- (22) Hanna, J. V.; Hart, R. D.; Healy, P. C.; Skelton, B. W.; White, A. H. *J. Chem. Soc., Dalton Trans.* **1998**, 2321–2325.
- (23) Effendy; Nicola, C. D.; Fianchini, M.; Pettinari, C.; Skelton, B. W.; Somers, N.; White, A. H. *Inorg. Chim. Acta* **2005**, *358*, 763–795.
- (24) Armarego, W. L.; Perrin, D. D. *Purification of Laboratory Chemicals*, 4th ed.; Butterworth-Heinemann Linacre House: Jordan Hill, Oxford, U. K., 1996.
- (25) Bashall, A.; Doyle, E. L.; Tubb, C.; Kidd, S. J.; McPartlin, M.; Woods, A. D.; Wright, D. S. *Chem. Commun.* **2001**, 2542–2543.
- (26) Brandys, M.; Jennings, M. C.; Puddephatt, R. J. *J. Chem. Soc., Dalton Trans.* **2000**, 4601–4606.
- (27) Tatsuno, Y.; Yoshida, T.; Otsuka, S. *Inorg. Synth.* **1990**, *28*, 342–343.
- (28) Furniss, B. S.; Hannaford, A. J.; Smith, P. W. G.; Tatchell, A. R. *Vogel's Textbook of Practical Organic Chemistry*, 5th ed.; ELBS: London, England, 1989; pp 428–429.
- (29) SMART, Version 5.625; Bruker-AXS: Madison, WI, 2000.
- (30) APEX2, version 2.1-0; Bruker-AXS: Madison, WI, 2006.
- (31) SAINT+, Version 7.03; Bruker-AXS: Madison, WI, 2006.
- (32) Sheldrick, G. W. SADABS, versions 2.05 and 2007/2; University of Göttingen: Göttingen, Germany, 2002.
- (33) SHELXTL, Version 6.10; Bruker-AXS: Madison, WI, 2000.